Arthritis Research & Therapy

RESEARCH

Open Access

Investigation of *GPM6B* as a novel therapeutic target in Osteoarthritis

Chongyang Feng[1†], Lin Liu[2†], Jinxue Zhang[1], Linxiao Wang[2], Ke Lv[3], Hongbo Li[3] and Yong Ding[3*]

Abstract

Background Osteoarthritis (OA) is the most common motor system disease in older people, characterized by a high incidence and significant social and economic burden. Women have a higher risk of OA, more severe clinical symptoms, and a higher rate of disabilities than men. However, the pathogenesis of OA remains unclear. Therefore, we screened for differentially expressed genes (DEGs) in OA patients of different sex and searched for new targets that may be involved in regulating the development of OA.

Methods The study compared the expression of DEGs in synovial fluid exosomes between male and female patients with OA through RNA sequencing combined with bioinformatics analysis using public data. To evaluate the screened DEGs, synovial tissue and fluid samples were obtained from patients with OA who underwent joint replacement surgery. SiRNA-mediated knockdown in vitro experiments were performed to investigate the role of glycoprotein membrane 6B (GPM6B). Meanwhile, GPM6B gene knockout mice were used to assess the in vivo pathological roles of GPM6B in OA.

Results The results revealed that GPM6B is a potential target associated with OA. Immunofluorescence staining demonstrated that GPM6B was expressed in fibroblast-like synoviocytes (FLS) and macrophage-like synoviocytes in patients with OA. In vitro experiments confirmed that *GPM6B* knockdown can reduce the expression of inflammatory factors in primary FLS from patients with OA. Under inflammatory conditions, *GPM6B* knockdown can reduce the expression of matrix metalloproteinases as well as proliferation of FLS. In addition, using a destabilization of the medial meniscus-induced OA model, we revealed that GPM6B is associated with OA progression in mice.

Conclusion Thus, we provided evidence that GPM6B act as a new target associated with OA.

Keywords Osteoarthritis, Sex, Fibroblast-like synoviocytes, Destabilization of the medial meniscus, Glycoprotein membrane 6B

†Chongyang Feng and Lin Liu contributed equally to this work.

*Correspondence:
Yong Ding
beijun2@sina.com
[1]Orthopedic Department of Tangdu Hospital, Fourth Military Medical University, Shaanxi, Xi'an 710038, China
[2]Department of Emergency, Honghui Hospital, Xi'an Jiaotong University, Shaanxi, Xi'an 710054, China
[3]Knee Preservation Division, Joint Surgery Department, Honghui Hospital, Xi'an Jiaotong University, Shaanxi, Xi'an 710054, China

Background

Osteoarthritis (OA) is a degenerative joint disease involving the cartilage and surrounding tissues, with the knee joint being the most common. It usually progresses slowly but may result in pain, joint failure, deformity, and disability, seriously affecting the quality of life of patients [1]. In clinical practice, only symptomatic treatment is available, and joint replacement surgery can be performed at the end stage, imposing a heavy economic burden on society and the patient's family [2, 3]. Pathological changes in OA are characterized by synovial inflammation, progressive destruction of the extracellular matrix, irreversible degradation of articular cartilage, and remodeling of subchondral bone [4, 5]. However, the precise mechanism of OA pathogenesis remains unclear.

Inflammation drives many pathological changes in OA, affecting the joint as a whole [6]. The inflammation in OA differs from that in rheumatoid arthritis and other autoimmune diseases because the former is chronic, comparatively low-grade, and mainly mediated mainly by innate immune responses [7]. Current therapies for OA, such as nonsteroidal anti-inflammatory drugs and hyaluronic acid, only control the symptoms, and no Food and Drug Administration-approved drugs are available for alleviating OA progression. However, studies have provided increasing insights into inflammatory mechanisms underlying OA, which are promising for the development of new therapeutic strategies [8, 9].

Glycoprotein membrane 6B (GPM6B) is a tetratransmembrane protein located on the human X-chromosome (Xq22.2), and belongs to the protein lipoprotein (PLP) family, along with GPM6A and PLP/DM20 [10]. GPM6B was initially demonstrated to be expressed in neurons, oligodendrocytes, and astrocytes [11]. Previous studies have revealed that GPM6B plays a role in smooth muscle cell differentiation, neuronal myelination, and neural cell functionality [12–14]; thus, it may further influence behavioral functions. The *GPM6B* mutant allele facilitates behavioral flexibility and enhances delay discounting; moreover, abnormal expression of GPM6A and GPM6B has been detected in the brains of depressed suicides, and X-chromosome genes, including *GPM6B*, have been linked to the genetic risk of Parkinson's disease [15–17]. It is also expressed in osteoblasts, where it plays a role in regulating osteoblast differentiation and mineralization [18]. In recent years, the role of GPM6B in tumors has been widely investigated. For example, one study identified GPM6B expression level as a predictor of favorable prognosis of patients with glioma; other studies have shown that GPM6B can mediate the plasticity of cancer stem cells and inhibit the proliferation of prostate cancer cells [10, 19, 20].

In this study, we speculated that *GPM6B* is a key gene that causes a higher incidence of OA. In addition, the role of GPM6B was verified by in vitro experiments and an in vivo OA mouse model. Our data provide new insights into the mechanisms of synovial inflammation in OA, and GPM6B may be a promising treatment target for OA.

Methods

Patients and samples

Synovial tissue and fluid samples were obtained from 11 male and 11 female patients with OA who underwent joint replacement surgery in the Orthopedic Department of Tangdu Hospital, Fourth Military Medical University. The ages of male and female patients were 65–77 and 61–72 years, respectively. Normal synovial tissue samples were obtained from 8 female and 8 male patients who underwent arthroscopic surgery for meniscus or ligament injury caused by trauma. The female patients were aged 20–28 years, and the male patients were aged 18–25 years. According to the institutional protocols (number: 20220923) approved by the Ethics Committee of the Tangdu Hospital of Fourth Military Medical University, written informed consent was obtained from all enrolled patients.

The inclusion criteria for patients with OA were as follows: (1) age > 18 years; (2) patients with knee OA who met the diagnostic criteria for OA established by the American College of Rheumatology; (3) those who underwent X-ray examination preoperatively and had a Kellgren–Lawrence grade of ≥III; and (4) those who underwent systematic conservative treatment preoperatively but showed no significant results. The exclusion criteria for patients with OA were as follows: (1) patients with ankylosing spondylitis or rheumatoid arthritis requiring joint replacement and (2) those with infected knee joints.

The inclusion criteria for control participants were as follows: (1) age > 18 years; (2) no joint pain symptoms before trauma, OA symptoms, or other types of arthritis; and (3) presence of acute trauma leading to meniscus or ligament injury in the knee joint (X-ray showing Kellgren–Lawrence grade of ≤I). The exclusion criteria for control participants were as follows: (1) individuals with infected knee joints and (2) those with other types of arthritis.

RNA sequencing (RNA-seq) of exosomes

Synovial fluid samples were collected from male and female patients with OA. Exosomes were prepared as described previously [21]. The size of exosomes was measured via nanoparticle tracking analysis (NTA; Saizhe Biotechnology; Guangzhou, China). The cup-shaped structure and particle size of exosomes were observed using transmission electron microscopy (TEM). Transcriptome sequencing of exosomes was performed by the

Saizhe Biological Company using Illumina high-throughput RNA-seq.

Data acquisition

Data used in this study were obtained from the public National Center for Biological Information. The database contains mRNA transcriptome data on OA synovial tissue and the patient's sex. Thus, three Gene Expression Omnibus (GEO) datasets were downloaded and used as verification sets: GSE12021 (eight female and two male patients), GSE55457 (eight female and two male patients), and GSE36700 (four female and one male patient). Transcriptomic analysis of the GEO dataset was performed using NetworkAnalyst (https://www.networkanalyst.ca/).

Culture of human primary fibroblast-like synoviocytes (FLS)

FLS were isolated from fresh synovial tissues in patients with OA. Briefly, after removing the adipose tissue, the synovial tissues were washed and sliced into small pieces, minced, and incubated in Dulbecco's modified Eagle's medium (DMEM; Gibco, USA) containing 0.15% collagenase II (Sigma-Aldrich, Burlington, MA, USA) at 37 °C for 2 h. After centrifugation, the upper liquid was discarded and 0.25% trypsin solution was added. The mixture was incubated at 37 °C for 20 min; then, an equal volume of DMEM (containing 20% FBS) was added to terminate digestion, followed by centrifugation. The upper liquid was discarded; finally, DMEM containing 20% FBS and 1% penicillin/streptomycin was added to the precipitate. The suspension was filtered through a 70-um cell sieve, and the filtrate was seeded into a culture dish at a desired cell density under standard conditions (37 °C, 5% CO_2). A trypsin–EDTA solution was used to remove the monolayer (confluency > 80%) above the cells, which were then passaged 3–5 times for use during the experiments. FLS were used within five passages in culture.

Immunofluorescence staining

Synovial tissues were fixed and embedded in paraffin and then sliced into 5-μm sections. The sections were dewaxed in xylene, rinsed in graded ethanol, rehydrated, and then rinsed again in phosphate-buffered saline (PBS). For high-temperature antigen retrieval, the sections were incubated with a citrate buffer solution (Maixin Bio; Fuzhou, China). The endogenous peroxidase activity was blocked with 3% H_2O_2, and unspecific binding was blocked with 5% bovine serum albumin (BSA). The following primary antibodies were used: mouse anti-human vimentin antibody (Boster Biological Technology; Wuhan, China), mouse anti-human CD68 antibody (Boster), and rabbit anti-human GPM6B antibody (Abcam; Cambridge, MA, USA). Incubation with primary antibodies was performed overnight at 4°C, followed by incubation with fluorescein isothiocyanate (FITC)–labeled goat anti-mouse and Cy3-labeled goat anti-rabbit secondary antibodies (MishuBio, Xi'an, China). For immunofluorescence staining, the primary FLS were fixed with 4% paraformaldehyde and permeabilized with 0.2% Triton X-100. The cells were then blocked with 5% BSA in PBS. To determine the purity of isolated FLS, the cells were incubated with the primary antibodies mouse anti-human vimentin antibody and rabbit anti-human CD68 antibody (Abcam), followed by incubation with FITC-labeled goat anti-rabbit and Cy3-labeled goat anti-mouse secondary antibodies (MishuBio). To detect GPM6B expression in isolated FLS, the cells were incubated at 4°C overnight with rabbit anti-human GPM6B antibody. After washing, the cells were incubated with FITC-labeled goat anti-rabbit secondary antibody. After final washing, the sections were mounted on slides with 4',6-diamidino-2-phenylindole-containing medium and observed under a fluorescence microscope (EVOS M5000; Life Technology).

Quantitative real-time polymerase chain reaction (qPCR)

Human synovial tissue samples were collected for cell isolation. Briefly, 50 mg of synovial tissue sample was placed in sterile and enzyme-free grinding tubes, and grinding beads were added. Then, 1 ml of TRIGene Reagent (GenStar, Beijing, China) was added to the tube and mixed; the grinding tube was placed in a precooled homogenizer, and grinding was performed by setting parameters according to the manufacturer's instructions. Then, the tissue homogenate was transferred to a new 1.5-ml Eppendorf tube, and the remaining steps were performed following the standard RNA extraction protocol. The RNA was reverse transcribed into cDNA using a reverse transcription kit (Yeasen, Shanghai, China). qPCR was performed using qPCR SYBR Green Master Mix (Yeasen). Transcript levels of target genes were normalized to the expression level of the housekeeping gene *GAPDH*.

qPCR analysis of FLS was performed following the standard protocols. Before the analysis, RNA concentration and purity were determined using Nanodrop 2000. All primers were purchased from Qingke Biotechnology (Beijing, China). The sequences used in qPCR are listed in Table 1.

Western blot

Western blot was performed using standard methods. Briefly, cells were lysed in RIPA buffer with protease inhibitor cocktail (Sigma-Aldrich), and proteins were quantified using the BCA protein assay kit (ThermoFisher, Carlsbad, CA, USA). Fifty micrograms of protein from each sample were loaded on SDS-PAGE, and

Table 1 List of primer sequences for qPCR

Gene	Forward (5′–3′)	Reverse (5′–3′)
GAPDH	AGAAGGCTGGGGCTCATTTG	AGGGGCCATCC ACAGTCTTC
GPM6B	GAGCCTCTCAATCAGACGGG	GCAGCCTTTTC TCTCTTGGC
MMP-1	ATGAAGCAGCCCAGATGTGGAG	TGGTCCACATCT GCTCTTGGCA
MMP-2	AGCGAGTGGATGCCGCCTTTAA	CATTCCAGGCA TCTGCGATGAG
MMP-9	GCCACTACTGTGCCTTTGAGTC	CCCTCAGAGA ATCGCCAGTACT
MMP-13	CCTTGATGCCATTACCAGTCTCC	AAACAGCTCCG CATCAACCTGC
IL-1β	GCTGAGGAAGATGCTGGTTC	GTGATCGTACA GGTGCATCG
IL-6	AGACAGCCACTCACCTCTTCAG	TTCTGCCAGTG CCTCTTTGCTG
TNF-α	AGGTCTACTTTGGGATCATTG	GGGGTAATAAA GGGATTGGG
ADATMS-5	TATGACAAGTGCGGACTATG	TTCAGGGCTAA ATAGGCAGT
COX-2	CGGTGAAACTCTGGCTAGACAG	GCAAACCGTAG ATGCTCAGGGA
VEGF	TTGCCTTGCTGCTCTACCTCCA	GATGGCAGTAG CTGCGCTGATA

Table 2 Oligonucleotide sequences of the siRNAs

Name	Sense (5′–3′)	Antisense (5′–3′)
siGPM6B-1	GUGUGGAUAUCCGACAAUATT	UAUUGUCGGAU AUCCACACTT
siGPM6B-2	CAACUUGUGAAGUCAUCAATT	UUGAUGACUUC ACAAGUUGTT
siGPM6B-3	GAUGCAGUAUGUCAUCUAUTT	AUAGAUGACAUA CUGCAUCTT

then proteins were transferred to PVDF membranes (Millipore, Bedford, MA, USA). Membranes were blocked with 5% BSA, and incubated overnight with the primary antibodies at 4 °C. Antibodies against matrix metalloproteinase (MMP)-1, MMP-2, MMP-3, MMP-9 and MMP-13 were purchased from Boster Biological Technology (Wuhan, China) and Santa Cruz Biotechnology (Santa Cruz, CA, USA). Then, membranes were washed with TBS and incubated with HRP-conjugated secondary antibody (ThermoFisher) in blocking buffer for 1 h at room temperature. After three washes, the proteins were visualized with enhanced chemiluminescence. To ensure the equal loading of protein, the blots were stripped and reprobed with an antibody against GAPDH. Protein bands were detected using a BIO-RAD imaging system (BIO-RAD, Hercules, CA, USA), and the band intensity was analyzed using the Image J software (NIH, Bethesda, MD, USA). Experiments were repeated three times.

Transfection of siRNA

Three siRNA sequences targeting *Gpm6b* were designed. The *Gpm6b* siRNAs (siGPM6B-1, siGPM6B-2, and siGPM6B-3), fluorescein amidite (FAM)-labeled negative control siRNA (siRNA-FAM), and negative control siRNA (NC) were synthesized by Qingke Biotechnology; the sequences are listed in Table 2. Human FLS were seeded into 24-well plates and cultured overnight before transfection. The cells were transfected with siRNA using the Lipofectamine 3000 reagent (Invitrogen; Carlsbad, CA, USA) according to the manufacturer's protocol. RNA and protein were isolated at 48 h following transfection.

Animal experiments

Gpm6b knockout (KO) mice with a C57BL/6 background were purchased from Cyagen Bioscience (Guangzhou, China). Wild-type (WT) C57BL/6 mice were purchased from the Animal Facility of the Fourth Military Medical University. Mice aged 8–10 weeks underwent sham or destabilization of the medial meniscus (DMM) surgery as previously described [22]. Briefly, a 3-mm skin incision was made under anesthesia over the medial aspect of the patellar ligament, followed by cutting the joint capsule into the femorotibial joint of the knee. To destabilize the anterior tibial plateau, the medial meniscotibial ligament was transected. Sham mice underwent the same surgical procedure without the transection of the medial meniscotibial ligament. Mice were sacrificed 8 weeks postoperatively. All experiments were performed following experimental protocols that had been approved by the Animal Care and Use Committee of our university.

Histopathology

The tissues were fixed in 4% (v/v) paraformaldehyde and decalcified using 10% (v/v) ethylenediaminetetraacetic acid. Then, the paraffin-embedded tissues were sliced into 5-μm thick sections. Hematoxylin and eosin (HE) and safranin O-fast green staining were performed. Based on HE staining, synovitis of mouse knee joints was scored (0–9) according to three synovial membrane features—synovial lining cell layer, inflammatory infiltrates, and stromal cell density—as follows: none (score: 0), slight (1), moderate (2), and strong (3) [23]. The cartilage damage and degeneration were graded using the Osteoarthritis Research Society International (OARSI) scoring system (0–6) based on safranin O-fast green staining [24]. The osteophyte size (0–3) and maturity (0–3) were scored according to a previous study [25].

5-ethynyl-2-deoxyuridine (EdU) proliferation assay

FLS were seeded into a 24-well plate, and EdU staining was conducted using the EdU Cell Proliferation Kit (RiboBio, Guangzhou, China) following the manufacturer's protocol. The cells were incubated with EdU (1:1000)

for 2 h. Subsequently, the cells were fixed with 4% paraformaldehyde and permeabilized with 0.5% Triton X-100. They were then incubated with Apollo solution for 30 min under dark conditions. Finally, the nuclei of the cells were stained with DAPI, and images were captured using a fluorescence microscope. EdU-positive cells were counted using statistical analysis.

Statistical analysis

Statistical analyses were performed using GraphPad Prism 9. Analysis used an unpaired *t*-test or one-way analysis of variance followed by Bonferroni post-hoc test. Nonparametric data were analyzed using the Kruskal–Wallis H test. *P*-values of <0.05 were considered to indicate statistical significance.

Results

Identification of *GPM6B* as an OA-related gene

Exosomes derived from the synovial fluid play an important role in the pathophysiology of OA [26]. In the OA joint, chondrocytes, synoviocytes, and immune cells can secrete exosomes that transmit pathogenic signals to each other. Therefore, we first collected synovial fluid samples from male and female patients with OA, after which exosomes were extracted and RNA-seq was conducted. NTA revealed that the particle size was mainly distributed between 80 and 200 nm, with the highest concentration obtained at a diameter of 152 nm. Morphological analysis of exosomes was performed using TEM, revealing a typical cup shape (data not shown). Transcriptome sequencing analysis revealed that exosomes from the synovial fluid of female patients with OA displayed significantly differentially expressed genes (DEGs), with 1256 genes upregulated and 670 genes downregulated, compared with those of male patients with OA, as demonstrated in the volcano plot and heatmap (Fig. 1A and B).

Next, three OA synovial tissue datasets were downloaded from the GEO database. By integrating and analyzing three datasets, 292 DEGs were identified between male and female patients with OA, including 216 upregulated and 76 downregulated genes. By intersecting these genes with the DEGs obtained from synovial fluid exosomes, we finally identified 10 upregulated and 6 downregulated genes (Fig. 1C; Table 3). Among them, the expression of *GPM6B* showed the most significant upregulation in OA. To verify whether *GPM6B* is a key gene associated with OA, synovial tissues were collected from male and female patients with OA and control participants to perform qPCR analysis. The results showed that compared with males, the expression of *GPM6B* was upregulated in the synovial tissue of females, both in control participants and patients with OA. Among females, the expression level of *GPM6B* in patients with OA was significantly upregulated compared with that in control participants (Fig. 1D). These results suggest that *GPM6B* is a key gene involved in the development of OA and contributes to the higher incidence of OA observed in women.

GPM6B is highly expressed in FLS of female patients with OA

The synovial membrane mainly consists of macrophage-like synoviocytes (MLS) and FLS, also known as "type A synoviocytes" and "type B synoviocytes," respectively. Synovitis plays an essential role in the pathogenesis of OA. We observed the expression of GPM6B in MLS and FLS of patients with OA. Double immunofluorescence staining of CD68/GPM6B and vimentin/GPM6B in OA synovial samples was performed to evaluate their colocalization, and the results demonstrated that GPM6B was expressed on both MLS and FLS (Fig. 2A). Primary FLS were also isolated from synovial tissues of female and male patients with OA. The cells were considered FLS if they were typically spindle-shaped and could be characterized by immunofluorescence staining using vimentin antibody; meanwhile, CD68 macrophage marker staining is rare (Additional file 1 A). Immunofluorescence staining revealed that *GPM6B* expression was higher in the FLS from female patients with OA than in those from male patients with OA (Fig. 2B). Furthermore, qPCR revealed that the relative mRNA expression level of *GPM6B* in females with OA was significantly higher than that in males with OA (Fig. 2C).

GPM6B knockdown decreases the inflammatory factor levels in FLS

To investigate the role of *GPM6B* in FLS, siRNA-mediated knockdown experiments were performed. Based on transfection using FAM-labeled siRNA, a transfection efficiency of $>85\%$ was observed in FLS 24 h post-transfection (Fig. 3A). *GPM6B* siRNAs had a significantly lower interference efficiency than the blank control and NC-siRNA groups. Among the three available siRNAs, siGPM6B-3 exhibited the best transfection efficiency (Fig. 3B).

After knocking down *GPM6B*, the relative expression levels of various inflammatory factors, such as interleukin (IL)-1β, IL-6, and tumor necrosis factor-α, were significantly decreased (Fig. 3C). Moreover, a disintegrin and metalloproteinase with thrombospondin motif (ADAMTS)-5 can degrade the extracellular cartilage matrix [27]. It showed a significantly decreased expression in this study; however, no significant difference was observed in the expression of cyclooxygenase-2 and vascular endothelial growth factor after *GPM6B* knockdown (Fig. 3D).

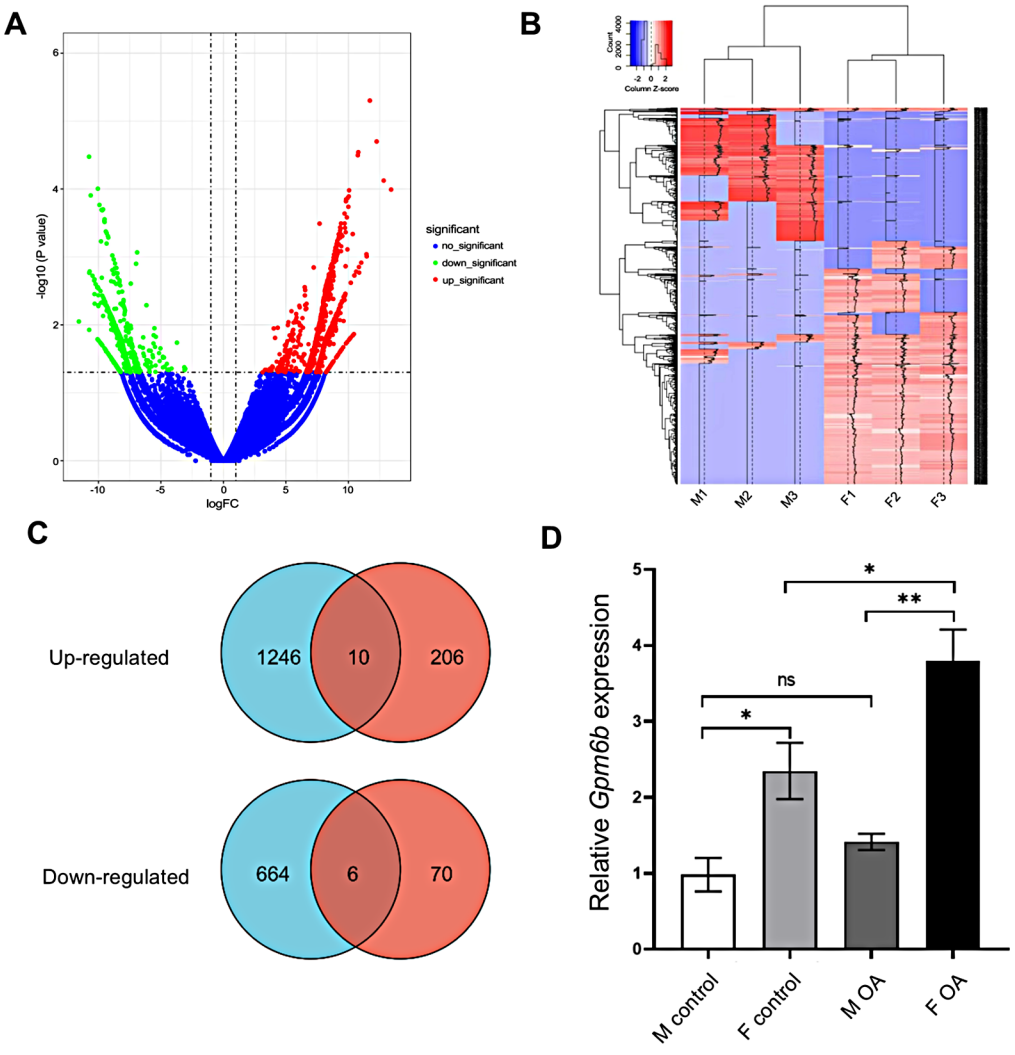

Fig. 1 Analysis and verification of *GPM6B* as an OA-related gene. (**A**) Volcanic map of mRNA differential expression in synovial exosomes of male and female patients with OA. Red dots represent upregulated genes, and blue dots represent downregulated genes. (**B**) Heat maps of mRNAs differentially expressed in synovial exosomes of male (**M**) and female (**F**) patients with OA, $n = 3$/group. (**C**) Venn diagram of co-upregulated/downregulated genes in exosomal RNA sequencing and GEO datasets in male and female patients with OA. Up: co-upregulated genes, down: co-downregulated genes; blue represents differentially expressed genes in synovial fluid exosomes of male and female patients with OA, whereas red represents differentially expressed genes in the synovial tissue of male and female patients with OA in the GEO datasets. (**D**) qPCR analysis of *GPM6B* expression. Human synovial tissue samples were collected from patients with OA and control participants, with each group comprising both male and female donors. * $P < 0.05$, ** $P < 0.01$; ns: no significant difference

GPM6B knockdown decreases MMP expression

FLS can mediate cartilage and bone destruction via MMPs. qPCR analysis revealed that compared to the blank control and NC-siRNA groups, *GPM6B* knockdown significantly reduced the mRNA expression levels of MMP-1, MMP-2, MMP-9, and MMP-13 in primary FLS isolated from patients with OA, whereas no significant effect was observed on MMP-3 expression levels (Fig. 4A). However, primary FLS stimulated with IL-1β significantly decreased the mRNA expression levels of all detected MMPs in the *GPM6B* siRNA group (Fig. 4B). Western blot results showed significantly decreased protein expression levels of MMP-3 and MMP-9 in IL-1β-stimulated primary FLS after *GPM6B* knockdown, while MMP-1, MMP-2 and MMP-13 showed a decreasing trend without statistical significance (Fig. 4C). These results indicate that GPM6B regulates MMP levels under physiologic inflammation.

Furthermore, the effects of GPM6B on the proliferation of primary OA-FLS were measured using the EdU assay. FLS exhibit tumor-like characteristics of uncontrolled proliferation, leading to increased and persistent inflammation [28, 29]. In turn, inflammatory cytokines induce the proliferation of FLS and promote the release of high levels of inflammatory cytokines, chemokines, and matrix-degrading enzymes [30]. As shown in Fig. 4D,

Table 3 Co-upregulated/downregulated differentially expressed genes in exosomal RNA sequencing and GEO datasets from male and female patients with OA

Gene	Log_2(FC)	*P* value	Up/Down
GPM6B	5.060912	0.004393	Up
CBFA2T3	4.877842	0.010513	Up
COL14A1	4.763199	0.018217	Up
KDM6A	4.617769	0.029939	Up
ZNF384	4.594071	0.031969	Up
ITGAL	4.588924	0.031969	Up
CNTLN	4.575978	0.033384	Up
IKBKB	4.528946	0.036257	Up
PUM2	4.504366	0.039841	Up
ARHGEF10	4.477159	0.043873	Up
PPP2R3C	−4.439623	0.048054	Down
UTY	−4.728519	0.020637	Down
DEF8	−4.784713	0.016451	Down
EIF5A	−4.793532	0.016291	Down
KDM5D	−5.299464	0.000568	Down
RPS4Y1	−6.381837	6.28E-12	Down

GPM6B knockdown inhibited cell proliferation, as evidenced by the significantly decreased number of EdU-positive FLS (Fig. 4D).

Lack of GPM6B attenuates synovial inflammation and cartilage degeneration in mice

To assess the in vivo pathological roles of GPM6B in OA, GPM6B KO mice were used. Homozygous mice were identified via tail-snip genotyping (Additional file 1B). Mice were born at the expected Mendelian ratio and exhibited no obvious developmental abnormalities (Additional file 1 C). In addition, a comparison of cartilage safranin O-fast green staining between WT and GPM6B KO mice showed no clear abnormalities or differences in both males and females (Additional file 2 A and 2B).

To induce the mouse model of OA, DMM surgery was performed in female mice. HE staining revealed that GPM6B KO mice exhibited less severe synovitis after DMM modeling compared to WT mice, as evidenced by reduced synovial hyperplasia, decreased inflammatory cell infiltration, and significantly lower synovitis scores (Fig. 5A). The OARSI score, osteophyte size, and osteophyte maturity were significantly higher in the DMM group than in the sham-operated controls. Compared with WT mice, GPM6B KO remarkably attenuated cartilage degradation (Fig. 5B) and significantly reduced OARSI score, osteophyte size, and osteophyte maturity (Fig. 5C-E). These data suggest that GPM6B knockdown attenuates synovial inflammation and cartilage degradation in OA.

Considering that sex plays an important role in OA pathology, *GPM6B* is a gene selected based on sex differences. Therefore, we further monitored male GPM6B KO mice after DMM surgery, revealing similar results (Fig. 6). These data further confirmed the effects of GPM6B on synovial inflammation and cartilage degradation in an OA model.

Discussion

Sex differences have been reported in OA prevalence and incidence. Women have a higher incidence of OA, more severe clinical symptoms, and a higher rate of disabilities, especially after menopause [31, 32]. The underlying reasons may be multifactorial, including hormonal issues, genetic factors, anatomical differences, and medical history [33]. Therefore, age, sex, obesity, joint injury, and genetic factors are the most common risk factors for OA [34].

Studies systematically reviewing preclinical studies have indicated that sex is an important risk factor for the development of OA; however, estrogen exerts many complex effects, indicating conflicting data. At the molecular level, the available data only indicate that inflammation is higher in females than in males, with limited information available on specific molecules, targets, and signaling pathways [35, 36]. A comprehensive study based on bioinformatics identified four co-upregulated and 10 co-downregulated genes and revealed that the enriched pathways differed between males and females. *BCL2L1*, *HNRNPD*, *PABPN1*, *EEF2*, *EEF1A1*, and *RPL37A* may be hub genes when considering sex-based differences in OA pathogenesis [37].

Herein, we evaluated sex differences in the expression of genes involved in OA. Synovial exosomes were collected from male and female patients with OA. After performing RNA-seq of exosomes, we screened out DEGs. Meanwhile, we downloaded data from the GEO public database, and 10 co-upregulated and 6 co-downregulated genes were identified. Among them, *GPM6B*, located on the X-chromosome, showed the most significant upregulation. Therefore, *GPM6B* was considered a potential target gene based on sex differences in OA development. qPCR was then performed to validate the expression of *GPM6B* in both male and female patients with OA and healthy controls. Consistent with bioinformatics analysis, qPCR analysis showed that the expression of *GPM6B* was significantly higher in female patients with OA.

Further investigations demonstrated that *GPM6B* knockdown in primary FLS significantly attenuated inflammatory factor levels. In addition, *GPM6B* knockdown decreased the expression of ADAMTS-5 in primary FLS. ADAMTS is a family of zinc ion-dependent metalloproteases. ADAMTS-5 (aggrecanase 2) is known to play a primary role in specific aggrecan degradation. Several studies have suggested that both ADAMTS-4 and ADAMTS-5 play important roles in human OA [38, 39].

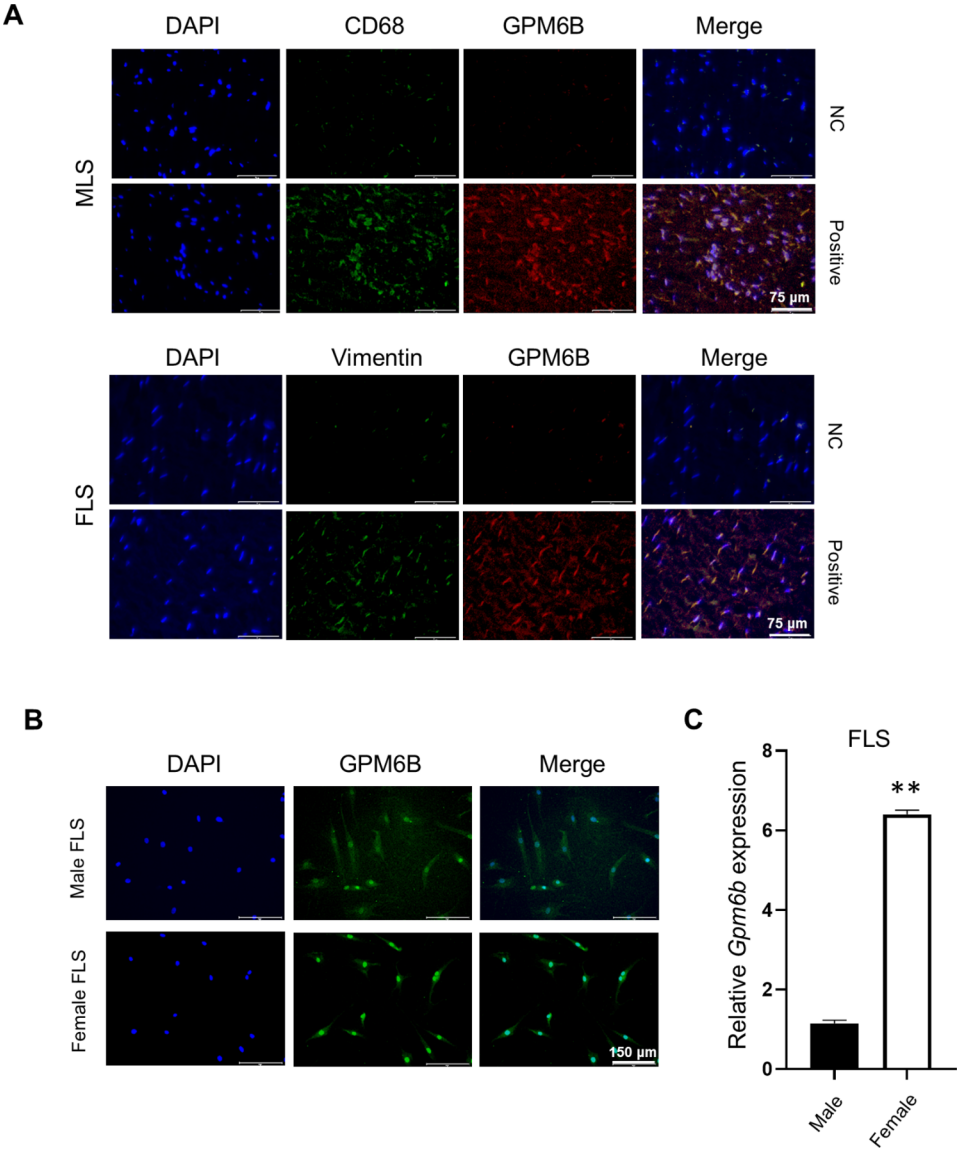

Fig. 2 GPM6B expression in the synovium of patients with OA. (**A**) Double immunofluorescence staining of CD68/GPM6B (upper panel) and vimentin/GPM6B (lower panel). CD68 and vimentin are markers for MLS and FLS, respectively. Negative control (NC), without primary antibodies; scale bars: 75 μm. (**B**) Immunofluorescence staining of GPM6B in primary FLS isolated from synovial tissues of female and male patients with OA; scale bars: 150 μm. (**C**) qPCR analysis of GPM6B levels in primary FLS isolated from synovial tissues of female and male patients with OA. Data are presented as the mean ± standard error, ** $P < 0.01$

The synovial membrane consists of the continuous surface layer of cells (intima) and underlying tissue (subintima). The intima comprises macrophages and fibroblasts, whereas the subintima includes blood vessels, fat cells, and fibroblasts, with few lymphocytes or macrophages. Fibroblasts can be isolated from the synovium, exhibiting the characteristics of mesenchymal stem cells (MSCs) after in vitro culture [40]. Therefore, these cells are considered synovium-derived MSCs. FLS can act as innate immune cells, releasing various immune regulatory cytokines, which are the most active cells in inflamed synovial tissues in early OA. Therefore, GPM6B exerts a regulatory effect on FLS; this finding is critical for expanding the perception of OA development and treatment.

In addition to inflammation-related factors, MMPs were investigated, which are considered biological markers of OA [41, 42]. MMP-3 and MMP-13 are most closely associated with the pathogenesis of knee OA [43]; and MMP-1 and MMP-13 play significant roles

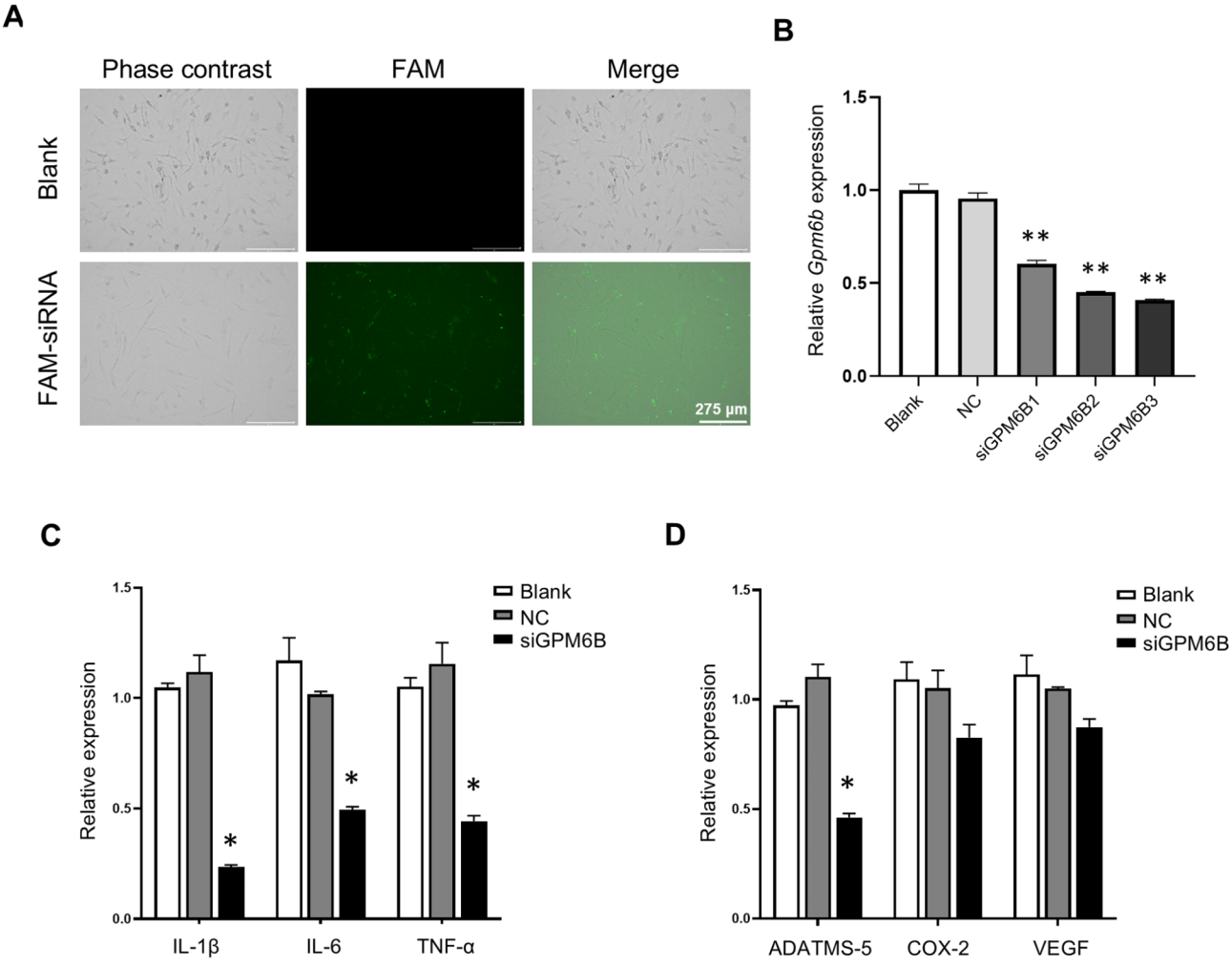

Fig. 3 GPM6B-regulated inflammatory factor levels in FLS. (**A**) siRNA transfection efficiency was measured via fluorescence microscopy using FAM-labeled scramble siRNA; scale bars: 275 μm. (**B**) qPCR quantification of the siRNA knockdown efficiency against GPM6B in FLS. Blank, control without transfection; negative control (NC) is transfected with scramble siRNA. (**C**) qPCR analysis of inflammatory factor levels in primary FLS; $n = 3$ per group. (**D**) qPCR analysis of ADATMS-5, COX-2, and VEGF levels in primary FLS isolated from synovial tissues of patients with OA; $n = 3$ per group. Data are presented as the mean ± standard error, * $P < 0.05$, ** $P < 0.01$ versus NC

in the degradation of the cartilage in OA [44]. MMP-2 and MMP-9 are gelatinases and contribute to the survival, proliferation, and migration of FLS in rheumatoid arthritis [42]. Both MMP-2 and MMP-9 are involved in inflammatory processes [45]. In the present study, MMP expression was significantly downregulated in *GPM6B* knockdown FLS, especially under IL-1β stimulation.

The beneficial effects of GPM6B knockdown were also confirmed in a mouse model of DMM OA. The lack of GPM6B alleviates synovitis and cartilage degeneration and reduces the severity of experimental OA both in female and male mice. From the beginning, we screened and proposed GPM6B as a sex-specific target in OA pathogenesis. Unexpectedly, in vivo experiments confirmed that GPM6B affects synovitis and cartilage degeneration regardless of the sex. We suggested two possible reasons for this result. First, the hindlimb weight-bearing function and joint stress of a quadrupedal animal are substantially different than those of bipedal humans [46]. Mice have a very thin cartilage layer, making it difficult to induce small defects that progress slowly [24]. It is commonly used for transgenic experimental models and for testing small animal models before transitioning to larger animals or clinical trials for human degenerative OA [47]. Thus, although DMM is a commonly used in vivo OA model, the differences in subsequent destruction during OA progression between female and male GPM6B KO mice may not be evident. Therefore, the relationship of GPM6B with OA disease progression and severity and with sex differences requires further research.

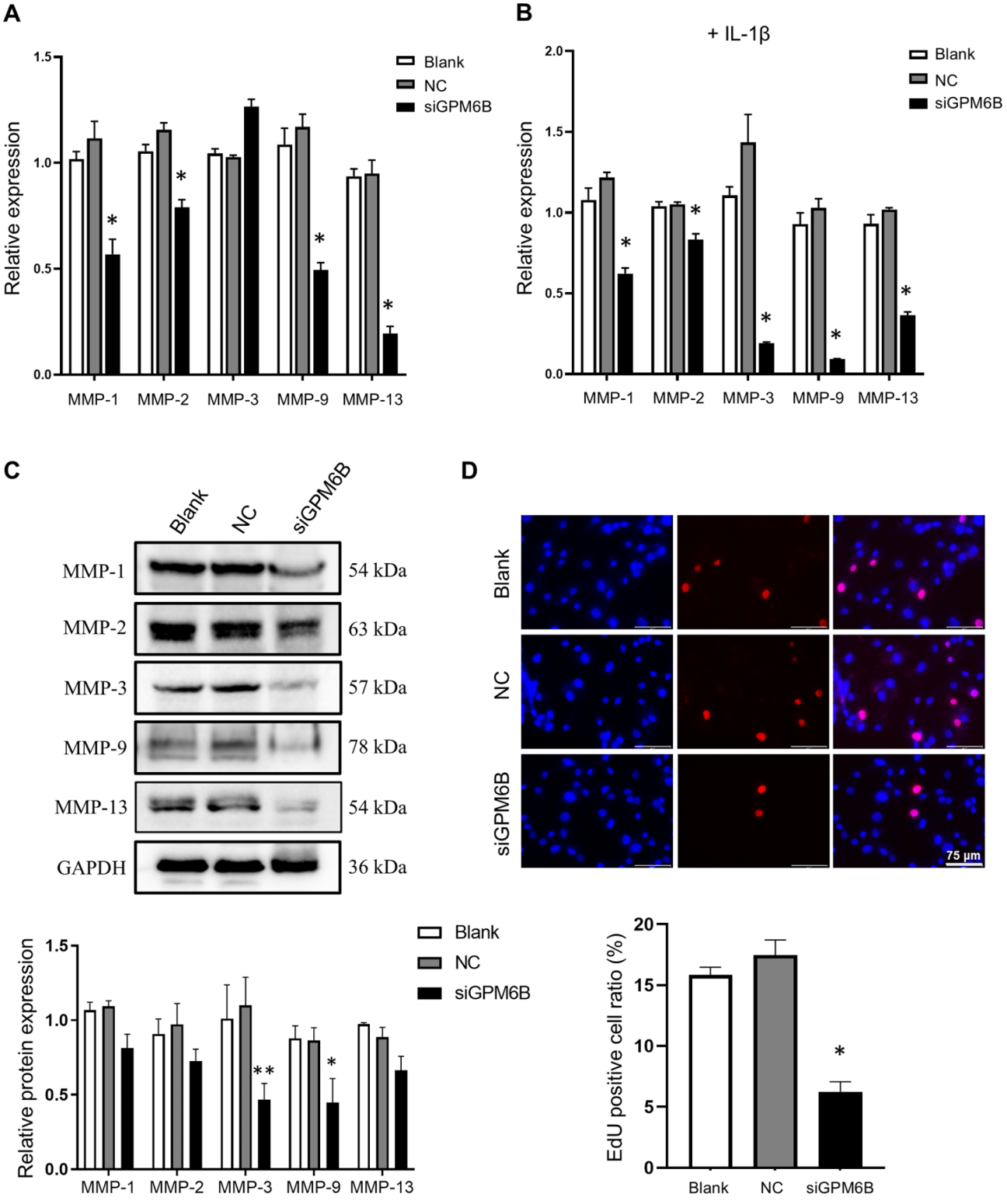

Fig. 4 GPM6B-regulated MMPs in FLS. (**A**) qPCR analysis of MMP levels in primary FLS without IL-1β stimulation. (**B**) qPCR analysis of MMP levels in primary FLS isolated from synovial tissues of patients with OA and IL-1β stimulation. (**C**) Western blot analysis of MMP levels in primary FLS with IL-1β stimulation. (**D**) EdU incorporation assay was used to evaluate FLS proliferation with IL-1β stimulation, and the cells were treated as indicated. $n = 3$ per group; scale bars: 75 μm. Data are presented as the mean ± standard error, * $P < 0.05$, ** $P < 0.01$ versus NC

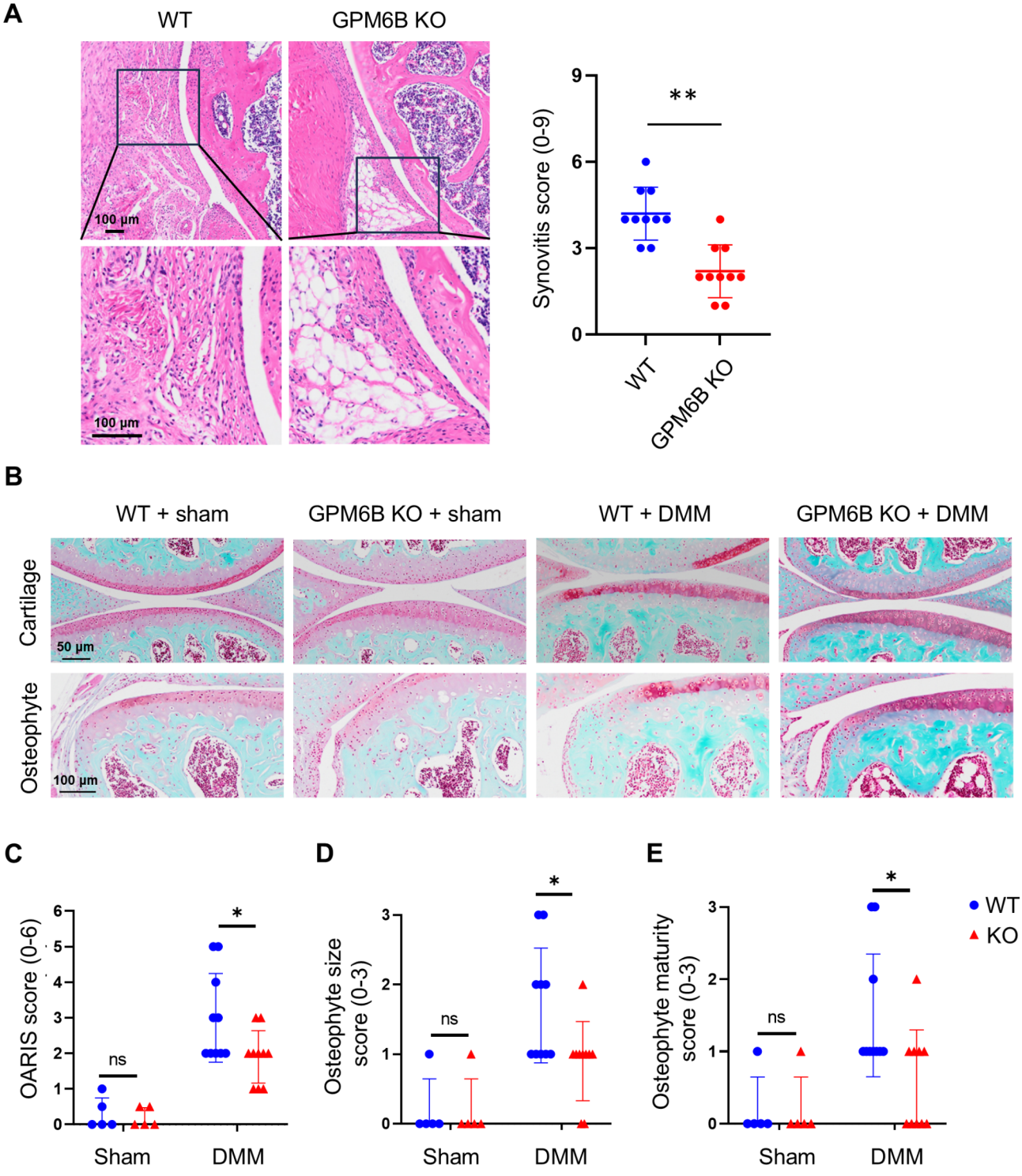

Fig. 5 Knee histopathology of female mice post-DMM. (**A**) Representative images and quantification of HE staining in the synovium of wild-type (WT) and GPM6B knockout (KO) mice at 8 weeks after DMM surgery. Scale bars: 100 μm. (**B**) Representative images of safranin O-fast green staining. Scale bars: 50 μm and 100 μm. (**C**) OARSI score. (**D**) Osteophyte size. (**E**) Osteophyte maturity. Data are presented as the mean ± standard deviation, * $P < 0.05$, ns: no significant difference

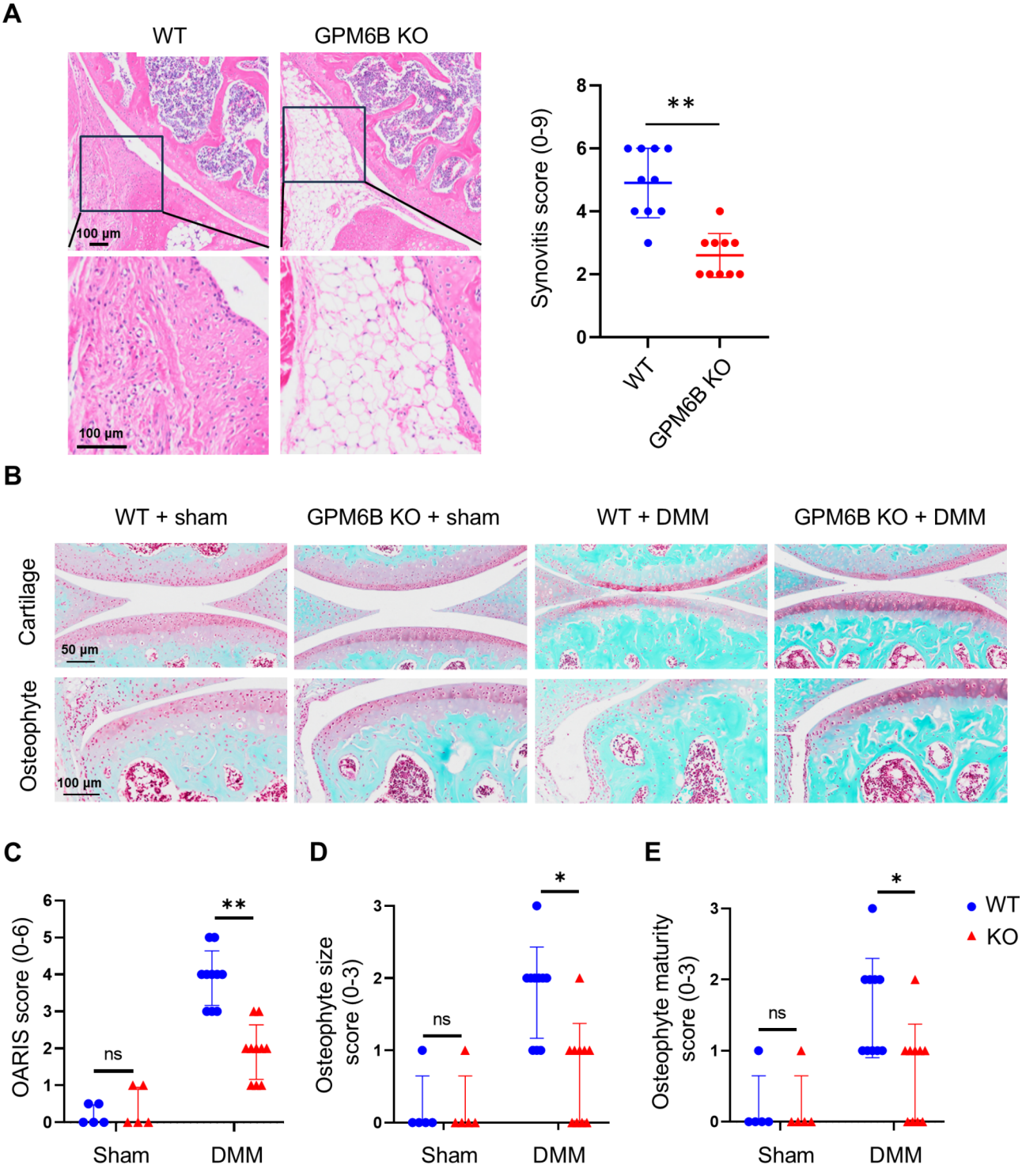

Fig. 6 Knee histopathology of male mice post-DMM. (**A**) Representative images and quantification of HE staining in the synovium of WT and GPM6B KO mice at 8 weeks after DMM surgery. Scale bars: 100 μm. (**B**) Representative images of safranin O-fast green staining. Scale bars: 50 μm and 100 μm. (**C**) OARSI score. (**D**) Osteophyte size. (**E**) Osteophyte maturity. Data are presented as the mean ± standard deviation, * $P < 0.05$, ** $P < 0.05$; ns: no significant difference

Conclusion

Here, we analyzed RNA-seq data obtained from OA synovial fluid exosomes and related public databases and revealed that GPM6B is linked to OA. In vitro studies showed that GPM6B regulates the expression of OA-related genes in FLS, thereby affecting synovitis and extracellular matrix components. In vivo studies demonstrated that GPM6B may exert a protective effect on mouse articular cartilage by improving synovitis. Therefore, these findings may provide a novel potential therapeutic target for OA.

Abbreviations

ADAMTS	A disintegrin and metalloproteinase with thrombospondin motif
BSA	Bovine serum albumin
DEGs	Differentially expressed genes
DMEM	Dulbecco's modified Eagle's medium
DMM	Destabilization of the medial meniscus
EdU	5-ethynyl-2-deoxyuridine
FAM	Fluorescein amidite
FITC	Fluorescein isothiocyanate
FLS	Fibroblast-like synoviocytes
GEO	Gene Expression Omnibus
GPM6B	Glycoprotein membrane 6B
HE	Hematoxylin and eosin
IL	Interleukin
KO	Knockout
MLS	Macrophage-like synoviocytes
MMP	Matrix metalloproteinase
MSCs	Mesenchymal stem cells
NC	Negative control
NTA	Nanoparticle tracking analysis
OA	Osteoarthritis
OARSI	Osteoarthritis Research Society International
PBS	Phosphate-buffered saline
PLP	Protein lipoprotein
qPCR	Quantitative real-time polymerase chain reaction
TEM	Transmission electron microscopy
WT	Wild-type

Supplementary Information

The online version contains supplementary material available at https://doi.org/10.1186/s13075-024-03430-6.

Supplementary Material 1

Supplementary Material 2

Acknowledgements

Not applicable.

Author contributions

CF and LL wrote the initial draft. CF, LL, JZ, LW, KL, and HL performed the experiments and data analysis. CF, LL, and YD assisted with the experimental design and data interpretation. CF and YD designed and administered the study and wrote the manuscript, which all authors commented on. All authors reviewed the manuscript critically for important intellectual content. All authors read and approved the final manuscript and agree to be accountable for the content.

Funding

Not applicable.

Data availability

Data used in this study were obtained from the public National Center for Biological Information. The database contains mRNA transcriptome data of OA synovial tissue and patient sex information. Thus, three Gene Expression Omnibus (GEO) datasets were downloaded and used as verification sets: GSE12021 (eight female and two male patients), GSE55457 (eight female and two male patients), and GSE36700 (four female and one male patient).

Declarations

Ethics approval and consent to participate

All experiments were performed following experimental protocols that had been approved by the Animal Care and Use Committee of our university. According to the institutional protocols (number: 20220923) approved by the Ethics Committee of the Tangdu Hospital of Fourth Military Medical University, written informed consent was obtained from all enrolled patients.

Consent for publication

Not applicable.

Competing interests

The authors declare no competing interests.

Received: 5 August 2024 / Accepted: 3 November 2024
Published online: 12 November 2024

References

1. Chaganti RK, Lane NE. Risk factors for incident osteoarthritis of the hip and knee. Curr Rev Musculoskelet Med. 2011;4(3):99–104.
2. Aspden RM, Saunders FR. Osteoarthritis as an organ disease: from the cradle to the grave. Eur Cell Mater. 2019;37:74–87.
3. Lopes EBP, Filiberti A, Husain SA, Humphrey MB. Immune contributions to Osteoarthritis. Curr Osteoporos Rep. 2017;15(6):593–600.
4. Yao Q, Wu X, Tao C, Gong W, Chen M, Qu M, et al. Osteoarthritis: pathogenic signaling pathways and therapeutic targets. Signal Transduct Target Ther. 2023;8(1):56.
5. Tong L, Yu H, Huang X, Shen J, Xiao G, Chen L, et al. Current understanding of osteoarthritis pathogenesis and relevant new approaches. Bone Res. 2022;10(1):60.
6. Loeser RF, Goldring SR, Scanzello CR, Goldring MB. Osteoarthritis: a disease of the joint as an organ. Arthritis Rheum. 2012;64(6):1697–707.
7. Robinson WH, Lepus CM, Wang Q, Raghu H, Mao R, Lindstrom TM, et al. Low-grade inflammation as a key mediator of the pathogenesis of osteoarthritis. Nat Rev Rheumatol. 2016;12(10):580–92.
8. Thysen S, Luyten FP, Lories RJ. Targets, models and challenges in osteoarthritis research. Dis Model Mech. 2015;8(1):17–30.
9. Farinelli L, Riccio M, Gigante A, De Francesco F. Pain Management Strategies in Osteoarthritis. Biomedicines. 2024;12(4).
10. Miao Z, Geng L, Xu L, Ye Y, Wu C, Tian W, et al. Integrated analysis reveals prognostic value and mesenchymal identity suppression by glycoprotein M6B in glioma. Am J Transl Res. 2022;14(5):3052–65.
11. Werner H, Dimou L, Klugmann M, Pfeiffer S, Nave KA. Multiple splice isoforms of proteolipid M6B in neurons and oligodendrocytes. Mol Cell Neurosci. 2001;18(6):593–605.
12. Zhang X, Xie H, Chang P, Zhao H, Xia Y, Zhang L, et al. Glycoprotein M6B interacts with TbetaRI to activate TGF-beta-Smad2/3 signaling and promote smooth muscle cell differentiation. Stem Cells. 2019;37(2):190–201.
13. Werner HB, Kramer-Albers EM, Strenzke N, Saher G, Tenzer S, Ohno-Iwashita Y, et al. A critical role for the cholesterol-associated proteolipids PLP and M6B in myelination of the central nervous system. Glia. 2013;61(4):567–86.
14. Bayat H, Mirahmadi M, Azarshin Z, Ohadi H, Delbari A, Ohadi M. CRISPR/Cas9-mediated deletion of a GA-repeat in human GPM6B leads to disruption of neural cell differentiation from NT2 cells. Sci Rep. 2024;14(1):2136.
15. Sanchez-Roige S, Barnes SA, Mallari J, Wood R, Polesskaya O, Palmer AA. A mutant allele of glycoprotein M6-B (Gpm6b) facilitates behavioral flexibility but increases delay discounting. Genes Brain Behav. 2022;21(4):e12800.
16. Fuchsova B, Alvarez Julia A, Rizavi HS, Frasch AC, Pandey GN. Altered expression of neuroplasticity-related genes in the brain of depressed suicides. Neuroscience. 2015;299:1–17.
17. Le Guen Y, Napolioni V, Belloy ME, Yu E, Krohn L, Ruskey JA, et al. Common X-Chromosome variants are Associated with Parkinson Disease Risk. Ann Neurol. 2021;90(1):22–34.

18. Drabek K, van de Peppel J, Eijken M, van Leeuwen JP. GPM6B regulates osteoblast function and induction of mineralization by controlling cytoskeleton and matrix vesicle release. J Bone Min Res. 2011;26(9):2045–51.
19. Kusumoto S, Ikeda JI, Kurashige M, Maeno-Fujinami E, Tahara S, Matsui T, et al. Tumor cell plasticity in endometrioid carcinoma is regulated by neuronal membrane glycoprotein M6-b. Oncol Lett. 2023;25(2):45.
20. He S, Huang Z, Li X, Ding Y, Sheng H, Liu B, et al. GPM6B inhibit PCa proliferation by blocking prostate Cancer Cell Serotonin Absorptive Capacity. Dis Markers. 2020;2020:8810756.
21. Song JE, Kim JS, Shin JH, Moon KW, Park JK, Park KS et al. Role of Synovial exosomes in Osteoclast differentiation in inflammatory arthritis. Cells. 2021;10(1).
22. Liu Y, Zhang Y, Zhang J, Ma J, Bian K, Wang Y, et al. CD226 is required to maintain Megakaryocytes/Platelets homeostasis in the treatment of knee osteoarthritis with platelet-rich plasma in mice. Front Pharmacol. 2021;12:732453.
23. Krenn V, Morawietz L, Burmester GR, Kinne RW, Mueller-Ladner U, Muller B, et al. Synovitis score: discrimination between chronic low-grade and high-grade synovitis. Histopathology. 2006;49(4):358–64.
24. Glasson SS, Chambers MG, Van Den Berg WB, Little CB. The OARSI histopathology initiative - recommendations for histological assessments of osteoarthritis in the mouse. Osteoarthritis Cartilage. 2010;18(Suppl 3):S17–23.
25. Little CB, Barai A, Burkhardt D, Smith SM, Fosang AJ, Werb Z, et al. Matrix metalloproteinase 13-deficient mice are resistant to osteoarthritic cartilage erosion but not chondrocyte hypertrophy or osteophyte development. Arthritis Rheum. 2009;60(12):3723–33.
26. Zhou Q, Cai Y, Jiang Y, Lin X. Exosomes in osteoarthritis and cartilage injury: advanced development and potential therapeutic strategies. Int J Biol Sci. 2020;16(11):1811–20.
27. Verma P, Dalal K. ADAMTS-4 and ADAMTS-5: key enzymes in osteoarthritis. J Cell Biochem. 2011;112(12):3507–14.
28. Smolen JS, Aletaha D, McInnes IB. Rheumatoid arthritis. Lancet. 2016;388(10055):2023–38.
29. Boehme KA, Rolauffs B. Onset and progression of human osteoarthritis-can Growth factors, inflammatory cytokines, or Differential miRNA expression concomitantly induce proliferation, ECM degradation, and inflammation in articular cartilage? Int J Mol Sci. 2018;19(8).
30. Park J, Ryu JH, Kim BY, Chun HS, Kim MS, Shin YI. Fermented lettuce extract containing nitric oxide metabolites attenuates inflammatory parameters in Model mice and in Human Fibroblast-Like synoviocytes. Nutrients. 2023;15(5).
31. O'Connor MI. Sex differences in osteoarthritis of the hip and knee. J Am Acad Orthop Surg. 2007;15(Suppl 1):S22–5.
32. Feng C, Zhang Y, Li W, Liu Y, Duan C, Ma J, et al. Identification of CaMK4 as a sex-difference-related gene in knee osteoarthritis. Ann Transl Med. 2023;11(5):194.
33. Palazzo C, Nguyen C, Lefevre-Colau MM, Rannou F, Poiraudeau S. Risk factors and burden of osteoarthritis. Ann Phys Rehabil Med. 2016;59(3):134–8.
34. Xiao P, Zhu X, Sun J, Zhang Y, Qiu W, Li J, et al. MicroRNA-613 alleviates IL-1beta-induced injury in chondrogenic CHON-001 cells by targeting fibronectin 1. Am J Transl Res. 2020;12(9):5308–19.
35. Srikanth VK, Fryer JL, Zhai G, Winzenberg TM, Hosmer D, Jones G. A meta-analysis of sex differences prevalence, incidence and severity of osteoarthritis. Osteoarthritis Cartilage. 2005;13(9):769–81.
36. Contartese D, Tschon M, De Mattei M, Fini M. Sex specific determinants in Osteoarthritis: a systematic review of Preclinical studies. Int J Mol Sci. 2020;21(10).
37. Yang Y, You X, Cohen JD, Zhou H, He W, Li Z, et al. Sex differences in Osteoarthritis Pathogenesis: a Comprehensive Study based on Bioinformatics. Med Sci Monit. 2020;26:e923331.
38. Zhao P, Liu D, Song C, Li D, Zhang X, Horecny I, et al. Discovery of Isoindoline Amide derivatives as potent and orally bioavailable ADAMTS-4/5 inhibitors for the treatment of Osteoarthritis. ACS Pharmacol Transl Sci. 2022;5(7):458–67.
39. Glasson SS, Askew R, Sheppard B, Carito B, Blanchet T, Ma HL, et al. Deletion of active ADAMTS5 prevents cartilage degradation in a murine model of osteoarthritis. Nature. 2005;434(7033):644–8.
40. Li F, Tang Y, Song B, Yu M, Li Q, Zhang C, et al. Nomenclature clarification: synovial fibroblasts and synovial mesenchymal stem cells. Stem Cell Res Ther. 2019;10(1):260.
41. Rousseau J, Garnero P. Biological markers in osteoarthritis. Bone. 2012;51(2):265–77.
42. Bryk M, Chwastek J, Mlost J, Kostrzewa M, Starowicz K. Sodium Monoiodoacetate dose-dependent changes in Matrix metalloproteinases and Inflammatory Components as prognostic factors for the progression of Osteoarthritis. Front Pharmacol. 2021;12:643605.
43. Milaras C, Lepetsos P, Dafou D, Potoupnis M, Tsiridis E. Association of Matrix Metalloproteinase (MMP) gene polymorphisms with knee osteoarthritis: a review of the literature. Cureus. 2021;13(10):e18607.
44. Wu YY, Li XF, Wu S, Niu XN, Yin SQ, Huang C, et al. Role of the S100 protein family in rheumatoid arthritis. Arthritis Res Ther. 2022;24(1):35.
45. Hannocks MJ, Zhang X, Gerwien H, Chashchina A, Burmeister M, Korpos E, et al. The gelatinases, MMP-2 and MMP-9, as fine tuners of neuroinflammatory processes. Matrix Biol. 2019;75–76:102–13.
46. To N, Curtiss S, Neu CP, Salgado CJ, Jamali AA. Rabbit trochlear model of osteochondral allograft transplantation. Comp Med. 2011;61(5):427–35.
47. Kim JE, Song DH, Kim SH, Jung Y, Kim SJ. Development and characterization of various osteoarthritis models for tissue engineering. PLoS ONE. 2018;13(3):e0194288.

Publisher's note